Electronic Supporting Information for

A solvent- and temperature-dependent intramolecular equilibrium of diamagnetic and paramagnetic states in Co complexes bearing triaryl amines

Linda Schnaubelt[a)], Holm Petzold[a)], Evgenia Dmitrieva[b)], Marco Rosenkranz[b)], Heinrich Lang[a)]*

a) Technische Universität Chemnitz, Faculty of Science, Institute for Chemistry, Inorganic Chemistry, 09107 Chemnitz, Germany. E-Mail: heinrich.lang@chemie.tu-chemnitz.de

b) Center of Spectroelectrochemistry, Leibniz Institute for Solid State and Materials Research (IFW Dresden), Helmholtzstr. 20, 01069 Dresden, Germany.

Content

1. Synthesis of triaryl amines

1.1. General Remarks

All reactions handling sensitive chemicals were carried out under an atmosphere of argon using standard Schlenk and cannula techniques. Anhydrous ethanol was purchased commercially from Acros Organics. Toluene was taken from a solvent purification system SPS-800 by MBraun. 2-(6-Bromopyridin-2-yl)-1,10-phenanthroline, **1a** and [Co(**1a**)$_2$](ClO_4)$_2$] were synthesised as previously reported in the literature.[1] All other chemicals were purchased from commercial suppliers and were used without further purification.

NMR spectra were recorded with a Bruker Avance III 500 spectrometer; chemical shifts for ^{1}H and ^{13}C NMR are referenced internally to the residual protons and to the ^{13}C NMR signal of the deuterated solvent. Elemental analyses were performed using a Thermo FlashAE 1112 analyser. Mass spectra were recorded with a Bruker micrOTOF-QIIa mass spectrometer operating in ESI mode (ESI = electrospray ionisation).

1.2. General synthesis of the triaryl amines

4-(Di-*p*-tolylamino)phenol was synthesised as reported in the literature.[2] However, triaryl amines with two or three methoxy groups could not be realised in the same way as 4-(di-*p*-tolylamino)phenol. Instead another reaction way was used which was modified from literature reports.[3,4] First (4-bromophenoxy)(*tert*-butyl)dimethylsilane was synthesised using *p*-bromophenol and dimethyl-*tert*-butylchlorosilane. After Buchwald-Hartwig coupling with the appropriate diaryl amines the hydroxyl group was deprotected using tetrabutylammonium fluoride (TBAF).

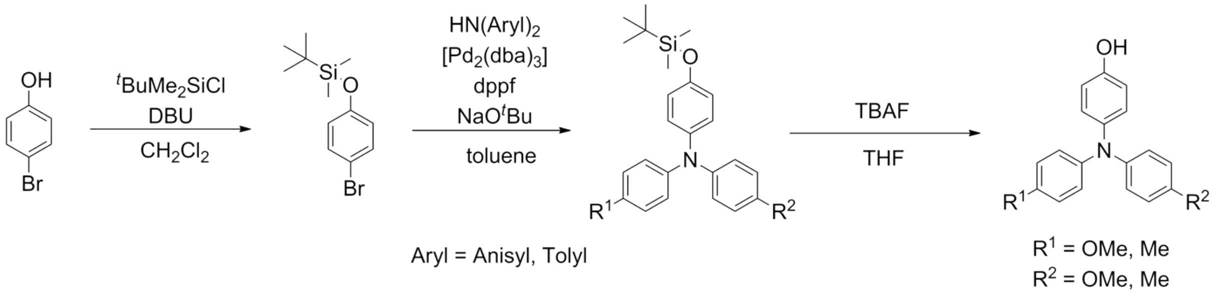

Scheme 1-SI *Synthetic route to hydroxyl-triarylamines (DBU = 1,8-diazabicyclo[5.4.0]unec-7-ene, dba = dibenzylideneacetone, dppf = 1,1'-bis(diphenylphosphino)ferrocene, TBAF = tetrabutylammonium fluoride).*

1.2.1. Synthesis of (4-bromophenoxy)(*tert*-butyl)dimethylsilane[5]

1 g (5.78 mmol) of *p*-bromophenol and 1.74 g (11.6 mmol) of *tert*-butylchlorodimethylsilane were dissolved in 30 mL of anhydrous dichloromethane. 2.27 mL (15 mmol) of 1,8-diazabicyclo[5.4.0]undec-7-ene (DBU) were added dropwise and the reaction mixture was stirred for 2 h at ambient temperature. The reaction progress was monitored by GC/MS. The solution was hydrolysed with water and extracted twice with an aqueous $NaHCO_3$ solution. The organic phase was dried over Na_2SO_4 and the dichloromethane was removed using a rotary evaporator. To remove the excess of *tert*-butylchlorodimethylsilane the oil was heated in oil pump vacuum at 50 °C for 4 h. 1.68 g of the title compound could be obtained as pale yellow oil (100 % based on *p*-bromophenol).

^{1}H NMR (500 MHz, $CDCl_3$, 298 K): 7.32 (d, J = 8.9 Hz, 2H), 6.71 (d, J = 8.9 Hz, 2H), 0.97 (s, 9H), 0.18 (s, 6H) ppm.

1.2.2. Synthesis of 4-((*tert*-butyldimethylsilyl)oxy)-*N*-(4-methoxyphenyl)-*N*-(*p*-tolyl)aniline

1.66 g (5.8 mmol) of (4-bromophenoxy)(*tert*-butyl)dimethylsilane, 2.5 g (11.6 mmol) of 4-methoxy-*N*-(*p*-tolyl)aniline, 0.106 g (2 mol-%) of [$Pd_2(dba)_3$], 0.13 g (4 mol-%) of dppf and 1.39 g (14.5 mmol) of sodium *tert*-butoxide were dissolved in 60 mL of anhydrous toluene and heated to 100 °C for 8 h. The reaction progress was monitored by GC/MS. After cooling the reaction mixture was hydrolysed with 100 mL of water and extracted with ethyl acetate and an aqueous $NaHCO_3$ solution. The combined organic phases were dried over $NaSO_4$ and all volatiles were removed in vacuum. The crude product was purified by column chromatography over SiO_2 (column size: 20 x 4 cm) using a mixture of *n*-hexane/ethyl acetate (97:3; v/v) as eluent. Yield: 1.59 g of a yellow oil (65 % based on (4-bromophenoxy)(*tert*-butyl)dimethylsilane).

EA calcd. for $C_{26}H_{33}NO_2Si$ (%): C 74.42, H 7.93, N 3.34; found: C 74.59, H 7.83, N 3.54. **^{1}H NMR** (500 MHz, $CDCl_3$, 298 K): 7.00 (dd, *J* = 8.6, 1.9 Hz, 4H), 6.92 (d, *J* = 8.8 Hz, 2H), 6.88 (d, *J* = 8.4 Hz, 2H), 6.80 (d, *J* = 9.0 Hz, 2H), 6.71 (d, *J* = 8.8 Hz, 2H), 3.78 (s, 3H), 2.28 (s, 3H), 0.98 (s, 9H), 0.19 (s, 6H) ppm. **^{13}C NMR** (125.8 MHz, $CDCl_3$, 298 K): 155.48, 151.17, 146.44, 142.15, 141.77, 130.78, 129.73, 125.97, 125.56, 122.34, 120.65, 114.70, 55.64, 25.84, 20.80, 18.32, –4.27 ppm. **MS-ESI**: 419.2275 ([M], calcd. 419.2281).

1.2.3. Synthesis of 4-((4-methoxyphenyl)(*p*-tolyl)amino)phenol

1.5 g (3.6 mmol) of 4-((*tert*-butyldimethylsilyl)oxy)-*N*-(4-methoxyphenyl)-*N*-(*p*-tolyl)aniline and 7.2 mL of a tetrabutylammonium fluoride solution (1 M in THF) were stirred in 40 mL of THF for 3 h. The reaction progress was monitored by GC/MS. After hydrolysing with water the mixture was extracted with CH_2Cl_2 and the combined organic phases were dried over Na_2SO_4. All volatiles were removed in vacuum. The crude product was purified by column chromatography over SiO_2 (column size: 20 x 4 cm) using a mixture of *n*-hexane/ethyl acetate (4:1; v/v) as eluent. 1.10 g of the title compound could be obtained as a yellow oil (100 % based on 4-((*tert*-butyldimethylsilyl)oxy)-*N*-(4-methoxyphenyl)-*N*-(*p*-tolyl)aniline).

EA calcd. for $C_{20}H_{19}NO_2 \cdot {}^1/_6\, H_2O$ (%): C 77.90, H 6.32, N 4.54; found: C 77.99, H 6.42, N 4.53. **^{1}H NMR** (500 MHz, $(CD_3)_2CO$, 298 K): 7.00 (dd, *J* = 8.7, 0.6 Hz, 2H), 6.96 (d, *J* = 9.1 Hz, 2H), 6.90 (d, *J* = 8.9 Hz, 2H), 6.85 (d, *J* = 9.1 Hz, 2H), 6.80 (d, *J* = 9.0 Hz, 2H), 6.78 (d, *J* = 8.6 Hz, 2H), 3.76 (s, 3H), 2.78 (s, 1H), 2.23 (s, 3H) ppm. **^{13}C NMR** (125.8 MHz, $(CD_3)_2CO$, 298 K): 156.48, 154.48, 147.61, 142.54, 141.25, 130.75, 130.36, 127.39, 126.41, 122.13, 116.90, 115.45, 55.72, 20.62 ppm. **MS-ESI**: 305.1410 ([M], calcd. 305.1416).

2. Principle of the intra- and intermolecular electron transfer

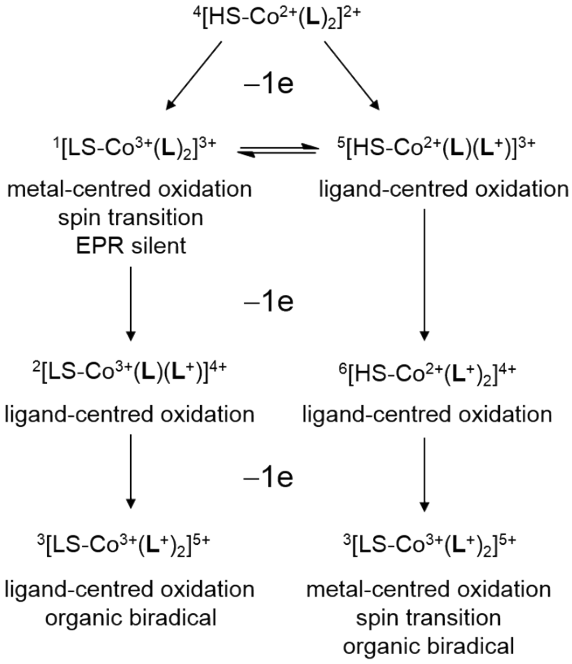

Scheme 2-SI *Overview of involved species upon oxidation of* $[\text{HS-Co}^{2+}(\mathbf{L})_2]^{2+}$ *(**L** = **1a**-**c**). The pathway is strongly solvent- and temperature-dependent. The oxidation of the ligand is always Tara-centred (Tara = triaryl amine). LS-Co*$^{2+}$ *species were not directly observed therefore they are not scheduled. HS = high-spin, LS = low-spin.*

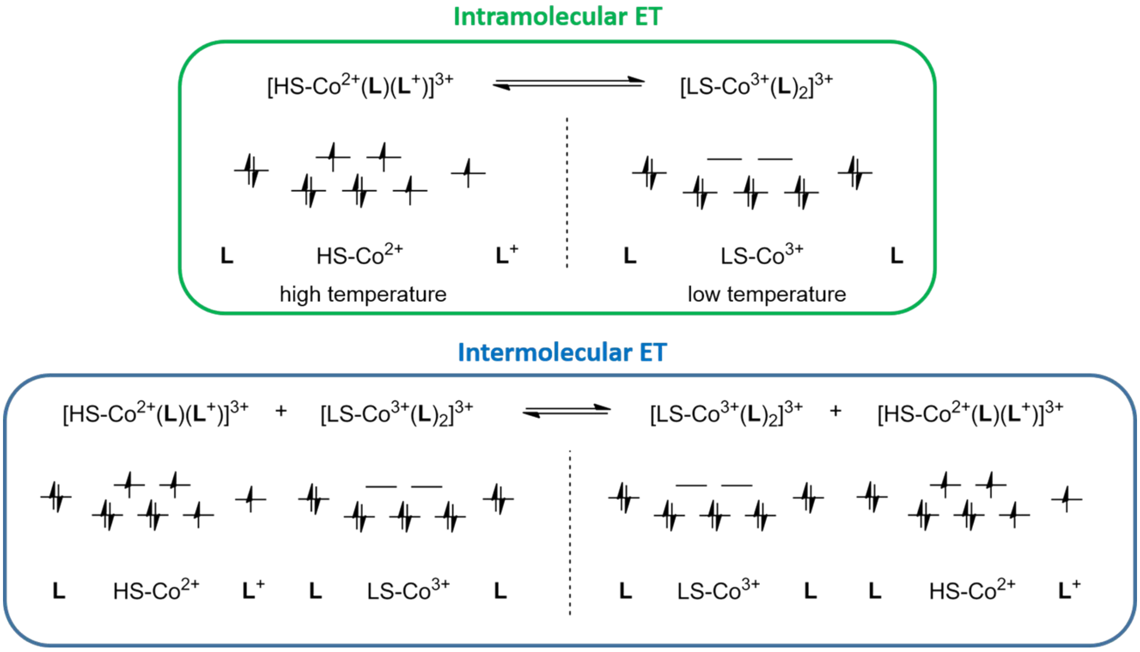

Scheme 3-SI *Principle of the discussed intra- and intermolecular electron transfer (ET) reactions in* $[\text{Co}(\mathbf{L})_2]^{3+}$ *(**L** = **1a**-**c**). HS = high-spin, LS = low-spin.*

3. Electrochemical measurements of [Co(**1a**-**c**)$_2$](ClO$_4$)$_2$

Electrochemical measurements on 1.0 mmol · L^{-1} solutions of the analyte in anhydrous acetonitrile and dichloromethane solutions containing 0.1 mol · L^{-1} of [N(^{n}Bu)$_4$][B(C$_6$F$_5$)$_4$] as supporting electrolyte were conducted under an atmosphere of argon at 25 °C utilising a Voltalab 10 electrochemical laboratory from Radiometer Analytical. A three electrode cell, which utilised a Pt auxiliary electrode, a glassy carbon working electrode (3 mm diameter) and an Ag/Ag$^+$ (0.01 M AgNO$_3$) reference electrode mounted on a Luggin capillary was used. The reference electrode was built from a silver wire inserted into a solution of 0.01 mol · L^{-1} [AgNO$_3$] and 0.1 mol · L^{-1} [N(^{n}Bu)$_4$][B(C$_6$F$_5$)$_4$] in acetonitrile, in a Luggin capillary with a Vycor tip. This Luggin capillary was inserted into a second Luggin capillary with a Vycor tip filled with a 0.1 mol · L^{-1} of [N(^{n}Bu)$_4$][B(C$_6$F$_5$)$_4$] in acetonitrile, propylene carbonate and dichloromethane, respectively.[6–10] The working electrode was prepared by polishing on a Buehler microcloth first with a 1 µm and then with a 1/4 µm diamond paste before every measurement. Successive experiments under same conditions showed that all formal oxidation and reduction potentials were reproducible within ±5 mV. Experimental potentials were referenced against an Ag/Ag$^+$ reference electrode but results are presented referenced against ferrocene (FcH/FcH$^+$ couple = 220 mV vs. Ag/Ag$^+$, ΔE_p = 61 mV) as an internal standard as required by IUPAC.[11–13] When decamethylferrocene [Fc* = Fe(η^5-C$_5$Me$_5$)$_2$] was used as an internal standard, the experimentally measured potential was converted into E vs. FcH/FcH$^+$ (under our conditions Fc*/Fc*$^+$ couple was at –513 mV vs. FcH/FcH$^+$, ΔE_p = 60 mV in acetonitrile). Data were then manipulated on a Microsoft Excel worksheet to set the formal redox potentials of the FcH/FcH$^+$ couple to E$^{0\prime}$ = 0.000 V. The cyclic voltammograms were taken after typical two scans and are considered to be steady state cyclic voltammetry in which the signal pattern differs not from the initial sweep. [^{n}Bu$_4$N][B(C$_6$F$_5$)$_4$] was prepared by metathesis of Li[B(C$_6$F$_5$)$_4$] · n Et$_2$O (Boulder Scientific) with [^{n}Bu$_4$N]Br according to the published procedure.[9]

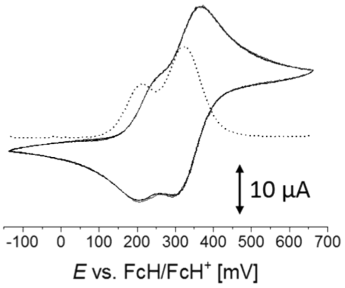

Figure 1-SI *Cyclic (solid) and square wave (dotted) voltammetry of [Co(**1c**)$_2$](ClO$_4$)$_2$ in CH$_3$CN at –5 °C. Measurement conditions: 1.0 mmol · L^{-1} analyte, [^{n}Bu$_4$N][B(C$_6$F$_5$)$_4$] (0.1 mol · L^{-1}) as supporting electrolyte, scan rate 100 mV · s^{-1} (CV) and 2 mV · s^{-1} (SWV), glassy carbon electrode.*

4. UV-vis-NIR spectroelectrochemical measurements of [Co(**1a**-**c**)$_2$](ClO$_4$)$_2$

Spectroelectrochemical measurements of 2.0 mmol L^{-1} anhydrous acetonitrile or dichloromethane solutions containing [Co(**1a-c**)$_2$](ClO$_4$)$_2$, and 0.1 mmol L^{-1} of [^{n}Bu$_4$N][B(C$_6$F$_5$)$_4$] as supporting electrolyte were performed in an OTTLE (optically transparent thin-layer electrochemistry, quartz window) cell[14] with a Varian Cary 5000 spectrophotometer utilising a Voltalab 10 potentiostat (Radiometer Analytical) at 25 °C. Between the spectroscopic measurements the applied potentials were increased in a step-wise manner using step heights of 25, 50, 100 or 200 mV. At the end of the measurements the analyte was reduced at –300 mV for 2 min and an additional spectrum was recorded to prove the reversibility of the oxidations.

Measurements in CH$_3$CN

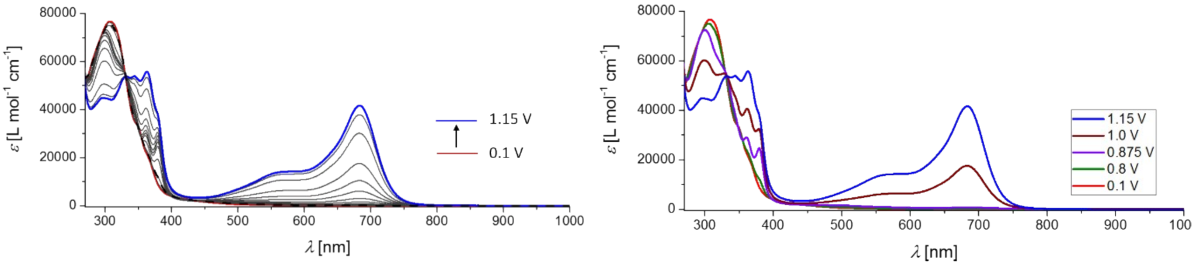

Figure 2-SI *[left] UV-vis-NIR spectra of [Co(**1a**)$_2$](ClO$_4$)$_2$ at rising potentials vs. Ag/AgCl in CH$_3$CN. The black dashed line is recorded after the series of measurements at –300 mV to prove the reversibility of the red absorption. [right] Potential dependence of absorption bands of [Co(**1a**)$_2$](ClO$_4$)$_2$. Measurement conditions: 2.0 mmol · L^{-1} analyte, [^{n}Bu$_4$N][B(C$_6$F$_5$)$_4$] (0.1 mol · L^{-1}) as supporting electrolyte, 25 °C.*

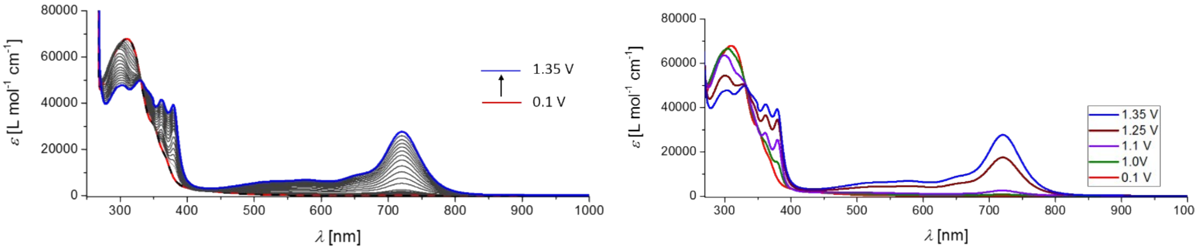

Figure 3-SI *[left] UV-vis-NIR spectra of [Co(**1b**)$_2$](ClO$_4$)$_2$ at rising potentials vs. Ag/AgCl in CH$_3$CN. The black dashed line is recorded after the series of measurements at –300 mV to prove the reversibility of the red absorption. [right] Potential dependence of absorption bands of [Co(**1b**)$_2$](ClO$_4$)$_2$. Measurement conditions: 2.0 mmol · L^{-1} analyte, [^{n}Bu$_4$N][B(C$_6$F$_5$)$_4$] (0.1 mol · L^{-1}) as supporting electrolyte, 25 °C.*

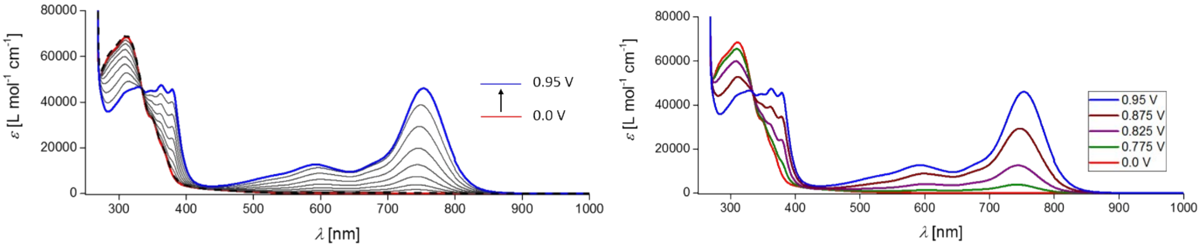

Figure 4-SI *[left] UV-vis-NIR spectra of [Co(**1c**)$_2$](ClO$_4$)$_2$ at rising potentials vs. Ag/AgCl in CH$_3$CN. The black dashed line is recorded after the series of measurements at –300 mV to prove the reversibility of the red absorption. [right] Potential dependence of absorption bands of [Co(**1c**)$_2$](ClO$_4$)$_2$. Measurement conditions: 2.0 mmol · L^{-1} analyte, [^{n}Bu$_4$N][B(C$_6$F$_5$)$_4$] (0.1 mol · L^{-1}) as supporting electrolyte, 25 °C.*

3.2. Measurements in CH_2Cl_2

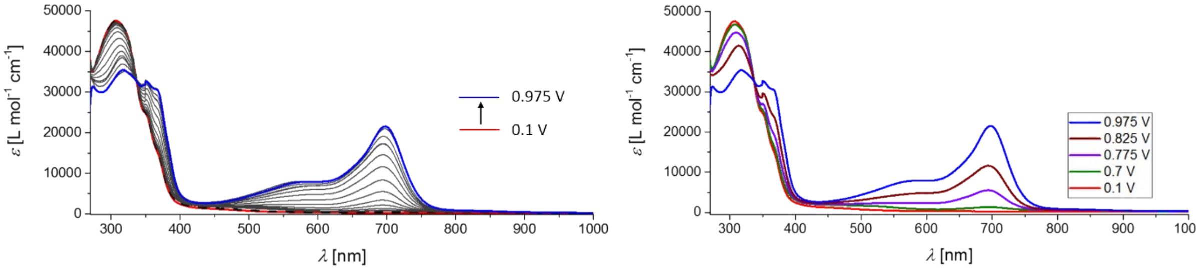

Figure 5-SI *[left] UV-vis-NIR spectra of [Co(**1a**)$_2$](ClO$_4$)$_2$ at rising potentials vs. Ag/AgCl in CH_2Cl_2. The black dashed line is recorded after the series of measurements at –300 mV to prove the reversibility of the red absorption. [right] Potential dependence of absorption bands of [Co(**1a**)$_2$](ClO$_4$)$_2$. Measurement conditions: 2.0 mmol · L^{-1} analyte, [^{n}Bu$_4$N][B(C$_6$F$_5$)$_4$] (0.1 mol · L^{-1}) as supporting electrolyte, 25 °C.*

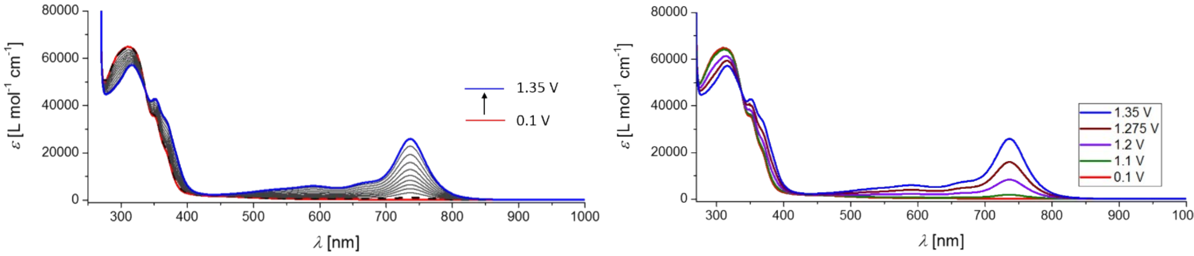

Figure 6-SI *[left] UV-vis-NIR spectra of [Co(**1b**)$_2$](ClO$_4$)$_2$ at rising potentials vs. Ag/AgCl in CH_2Cl_2. The black dashed line is recorded after the series of measurements at –300 mV to prove the reversibility of the red absorption. [right] Potential dependence of absorption bands of [Co(**1b**)$_2$](ClO$_4$)$_2$. Measurement conditions: 2.0 mmol · L^{-1} analyte, [^{n}Bu$_4$N][B(C$_6$F$_5$)$_4$] (0.1 mol · L^{-1}) as supporting electrolyte, 25 °C.*

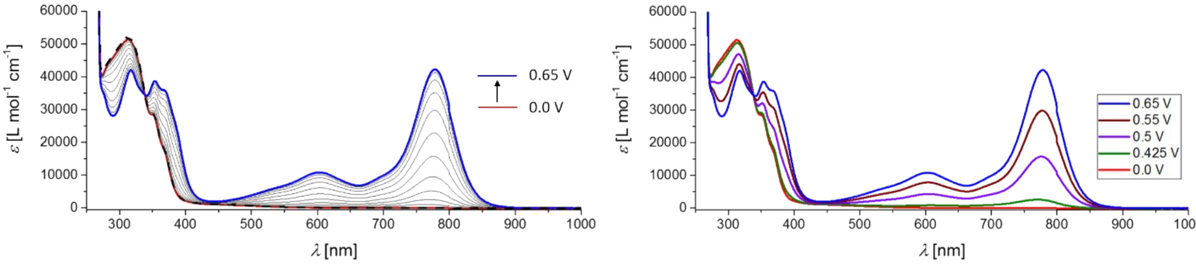

Figure 7-SI *[left] UV-vis-NIR spectra of [Co(**1c**)$_2$](ClO$_4$)$_2$ at rising potentials vs. Ag/AgCl in CH_2Cl_2. The black dashed line is recorded after the series of measurements at –300 mV to prove the reversibility of the red absorption. [right] Potential dependence of absorption bands of [Co(**1c**)$_2$](ClO$_4$)$_2$. Measurement conditions: 2.0 mmol · L^{-1} analyte, [^{n}Bu$_4$N][B(C$_6$F$_5$)$_4$] (0.1 mol · L^{-1}) as supporting electrolyte, 25 °C.*

5. VT vis-NIR spectroscopy of $[\mathrm{Co}(\mathbf{1a,c})_2]^{3+}$

VT (variable temperature) vis-NIR spectra were recorded with an Avantes AvaSpec-128 spectrometer and the AvaSoft8 software. Avantes AvaLight-Hal was used as light source.

The spectra of $[\mathrm{Co}(\mathbf{1a})_2]^{3+}$ (1 mmol · L^{-1}) were obtained in anhydrous dichloromethane solutions. The two ends of the illuminating and receiving fibre optic cables were connected to a self-made cuvette holder which was placed in a dewar vessel and cooled with liquid nitrogen. The temperature was monitored by a cryogenic temperature controller (Stanford Research Systems CTC100). $[\mathrm{Co}(\mathbf{1a})_2]^{3+}$ was obtained by adding 1 eq of $[\mathrm{N}(p\text{-}\mathrm{C_6H_5Br})_3][\mathrm{SbCl_6}]$ ("magic blue", Sigma-Aldrich) to $[\mathrm{Co}(\mathbf{1a})_2](\mathrm{ClO_4})_2$ in $\mathrm{CH_2Cl_2}$.

VT vis-NIR spectra of $[\mathrm{Co}(\mathbf{1c})_2]^{3+}$ (0.12 mmol · L^{-1}) were obtained in anhydrous acetonitrile solutions. The two ends of the illuminating and receiving fibre optic cables were connected to a transmission dip probe (Avantes) which was placed into a Schlenk tube containing the examined solution. The sample was cooled with a liquid nitrogen-ethanol bath and heated with a water bath. The temperature was monitored with an ordinary thermometer. $[\mathrm{Co}(\mathbf{1c})_2]^{3+}$ was obtained by adding 1 eq of magic blue to $[\mathrm{Co}(\mathbf{1c})_2](\mathrm{ClO_4})_2$ in $\mathrm{CH_3CN}$.

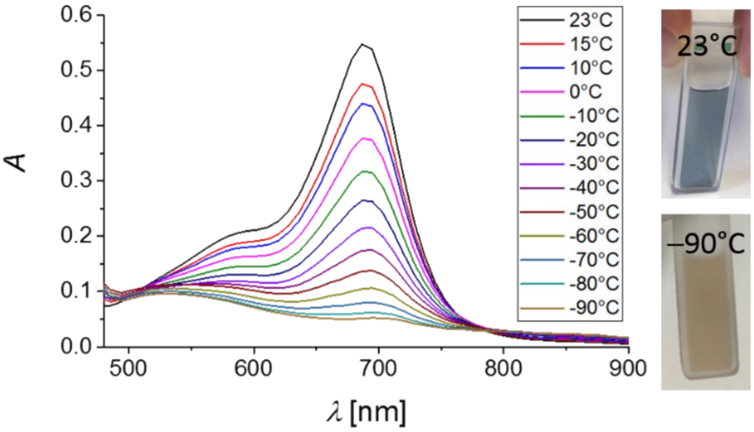

__Figure 8-SI__ Vis-NIR spectra of $[\mathrm{Co}(\mathbf{1a})_2]^{3+}$ *in* $\mathrm{CH_2Cl_2}$ *at given temperatures. The solution is blue coloured at T = 23 °C and yellow coloured at T = –90 °C.*

6. EPR/UV-vis-NIR spectroelectrochemistry of [Co(**1a**,**c**)$_2$](ClO$_4$)$_2$

The EPR/UV-vis-NIR spectroelectrochemical technique was described earlier.[15] For EPR measurements, an EMX X-band CW spectrometer (Bruker BioSpin, Germany) was used. The EPR spectra were registered at a microwave power of 5 mW and 100 kHz modulation. The EPR spectra were recorded in an optical EPR cavity (4104OR, Bruker, Germany) allowing the connection of two optical wave guides to measure *in situ* the electronic absorption spectra in the transmission mode simultaneously with the EPR spectra. For UV-vis-NIR measurements, the spectrometers AvaSpec-2048x14-USB2 with the CCD detector and AvaSpec-NIR256-2.2 with the InGaAs detector (Avantes, The Netherlands) applying the AvaSoft7.5 software were used. For the *in situ* experiments a balanced deuterium-halogen lamp AvaLight-DH-S-BAL serves as the light source. The *in situ* spectroelectrochemical measurements were controlled by a PG 390 potentiostat/galvanostat (HEKA Elektronik GmbH, Germany) equipped with the PotMaster v2x80 software, triggering both the EPR and UV-vis-NIR spectrometer modules. Experiments at different temperatures were performed with an internal variable temperature controller.

The spectroelectrochemical experiments were carried out in an EPR flat cell with a three-electrode arrangement consisting of a gold-µ-mesh (99.9 %, Goodfellow, UK) as the working electrode, a silver chloride-coated silver wire as the pseudo-reference electrode, and a platinum wire as the counter electrode. The potentials are referenced against ferrocene (FcH/FcH$^+$) couple. The EPR and vis-NIR spectra were collected at a continuous potential sweep rate of 5 mV · s^{-1}. Each vis-NIR spectrum was collected relative to that of the neutral compound at the initial potential.

The concentration of the samples was 1 mM. Solutions of 0.1 M [N(^{n}Bu)$_4$][B(C$_6$F$_5$)$_4$][6,16] in acetonitrile (99.8 %, anhydrous, Sigma-Aldrich) and dichloromethane (≥99.9 %, puriss. p.a., ACS reagent) were used as electrolyte. The electrolyte was deaerated by nitrogen bubbling. The preparation of the solutions was done in a glove box under inert atmosphere.

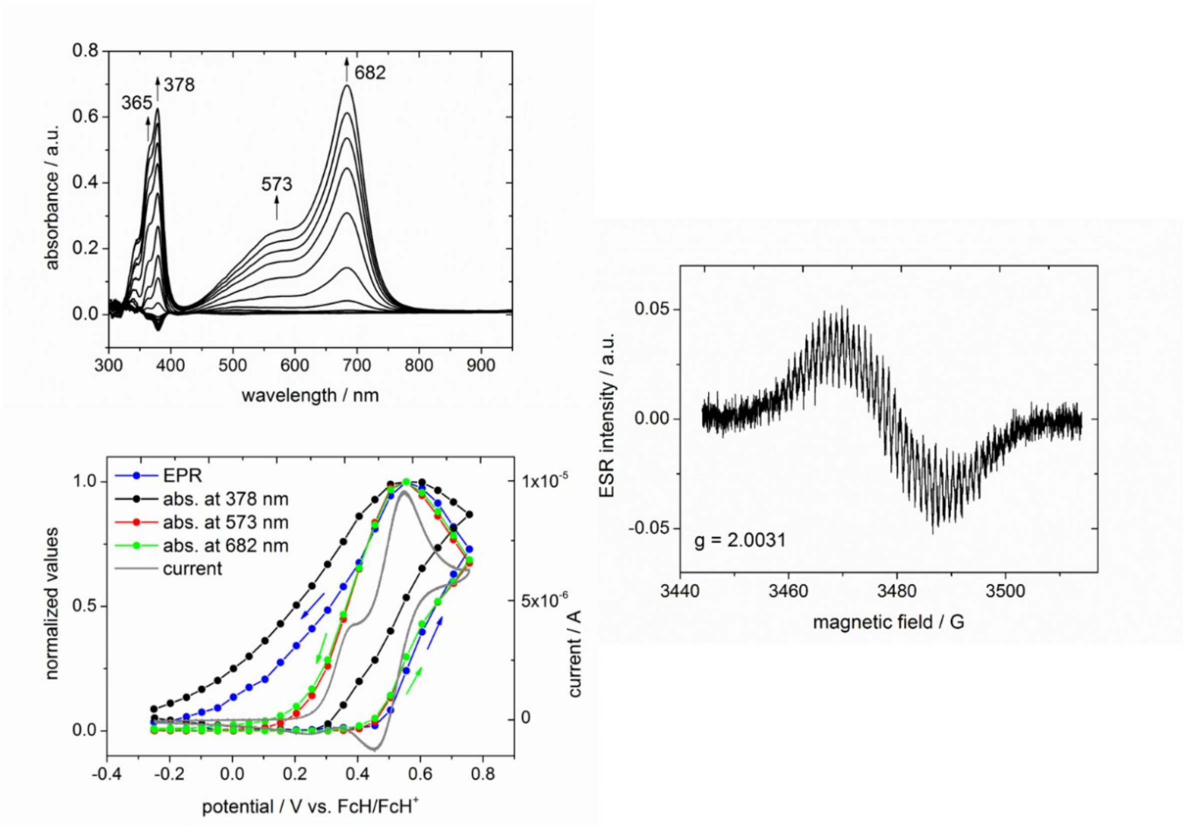

Figure 9-SI *[top left] In situ absorption spectra of [Co(**1a**)$_2$](ClO$_4$)$_2$ in CH$_3$CN at rising potentials. [bottom left] CV, potential dependence of the absorption bands and EPR intensity. [right] EPR spectrum at T = 298 K.*

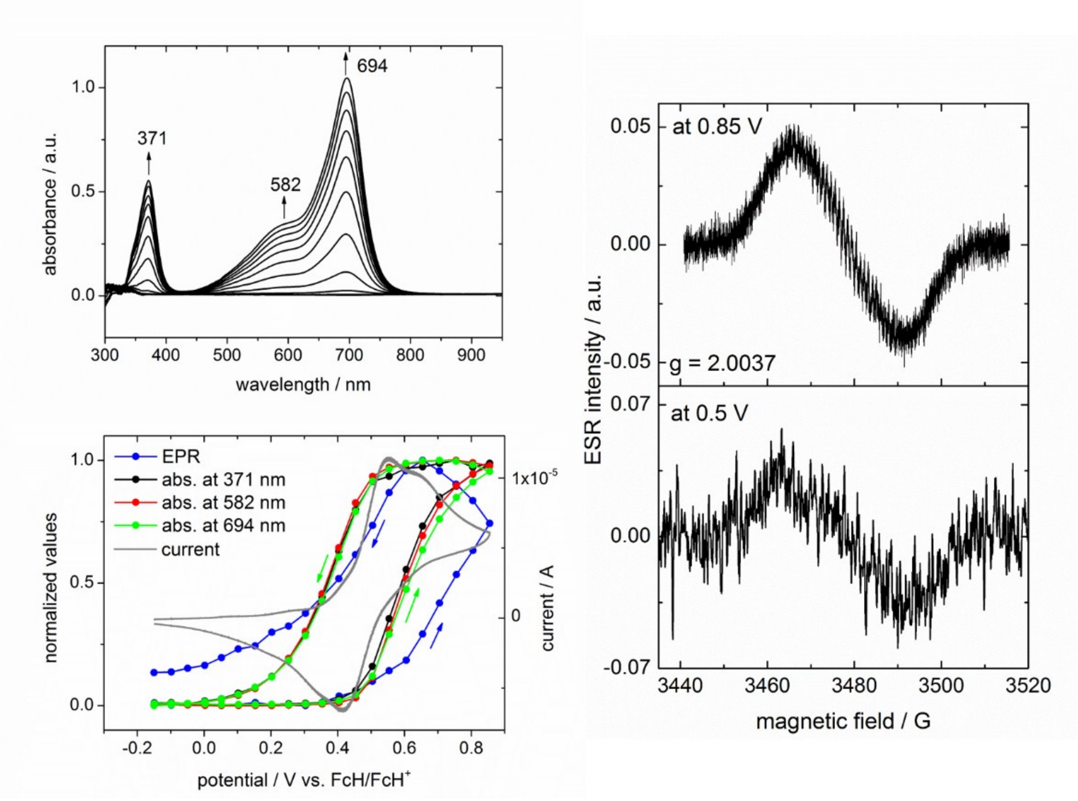

Figure 10-SI *[top left] In situ absorption spectra of [Co(**1a**)$_2$](ClO$_4$)$_2$ in CH$_2$Cl$_2$ at rising potentials. [bottom left] CV, potential dependence of the absorption bands and EPR intensity. [right] EPR spectra at E = 0.5 V and E = 0.85 V (T = 298 K).*

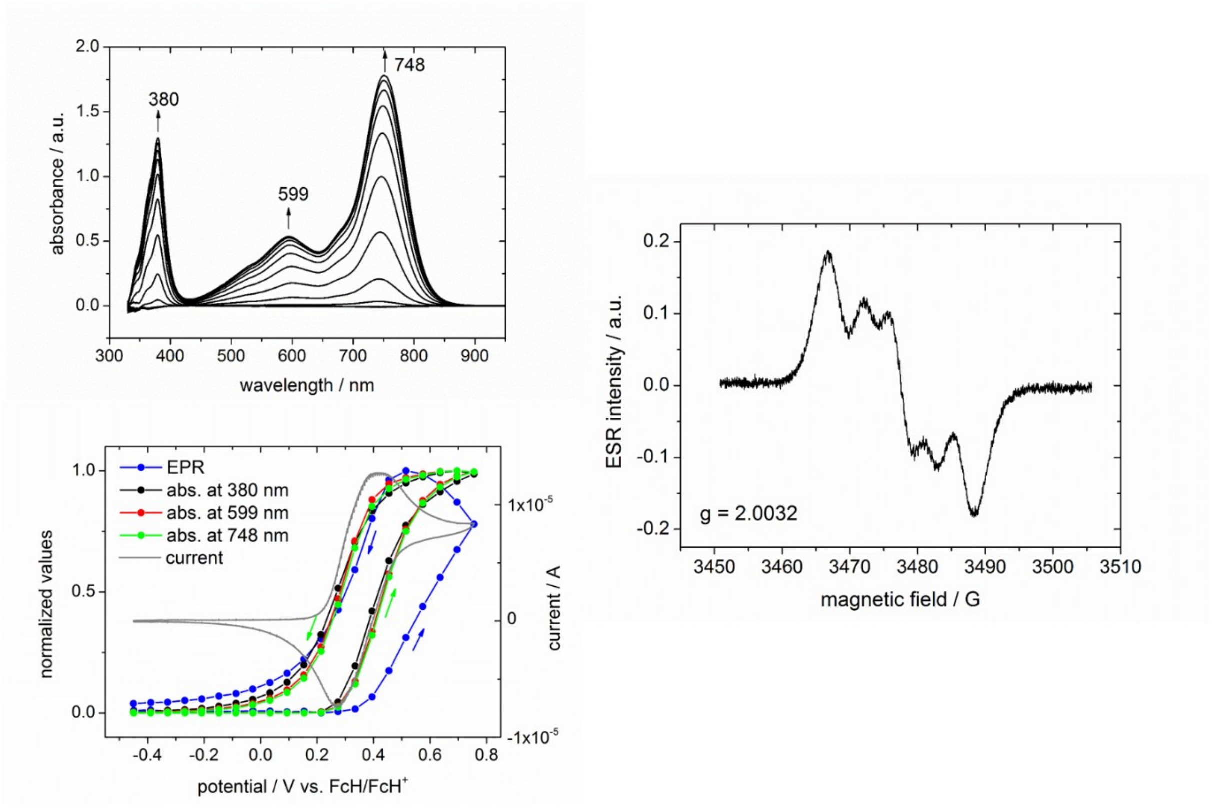

Figure 11-SI *[top left] In situ absorption spectra of [Co(**1c**)$_2$](ClO$_4$)$_2$ in CH$_3$CN at rising potentials. [bottom left] CV, potential dependence of the absorption bands and EPR intensity. [right] EPR spectrum at T = 298 K.*

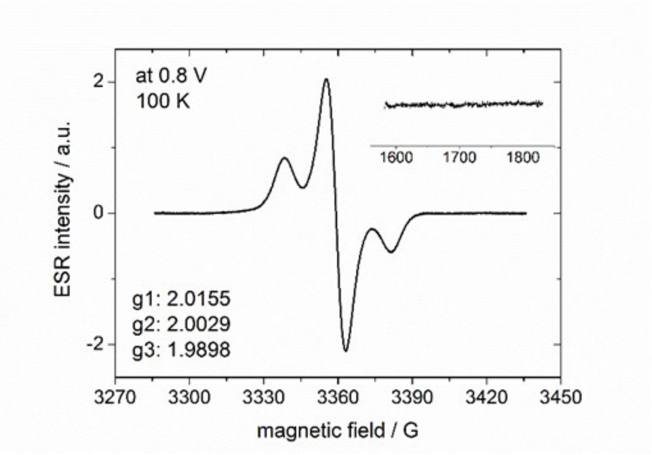

Figure 12-SI EPR spectrum of in situ generated [Co^{3+}(**1c**$^+$)$_2$]$^{5+}$ in CH$_3$CN at E = 0.8 V (T = 100 K). The inset shows the spectrum at half-field.

7. NMR spectroscopy of [Co(**1a**-**c**)$_2$](ClO$_4$)$_2$

NMR spectra were recorded with a Bruker Avance III 500 spectrometer including a TopSpin 2.1 programme package for data acquisition. Chemical shifts are referenced internally to the residual protons (d_1-chloroform δ = 7.26 ppm, d_3-acetonitrile δ = 1.94 ppm, d_6-acetone δ = 2.05 ppm) and to the ^{13}C NMR signal (d_1-chloroform δ = 77.16 ppm) of the deuterated solvent.[17] For the oxidation experiments [N(p-C_6H_4Br)$_3$][SbCl$_6$] ("magic blue", Sigma-Aldrich) was added with a sub-stoichiometric amount (≈ 0.5 eq) to a d_6-acetone solution containing [Co(**1c**)$_2$](ClO$_4$)$_2$.

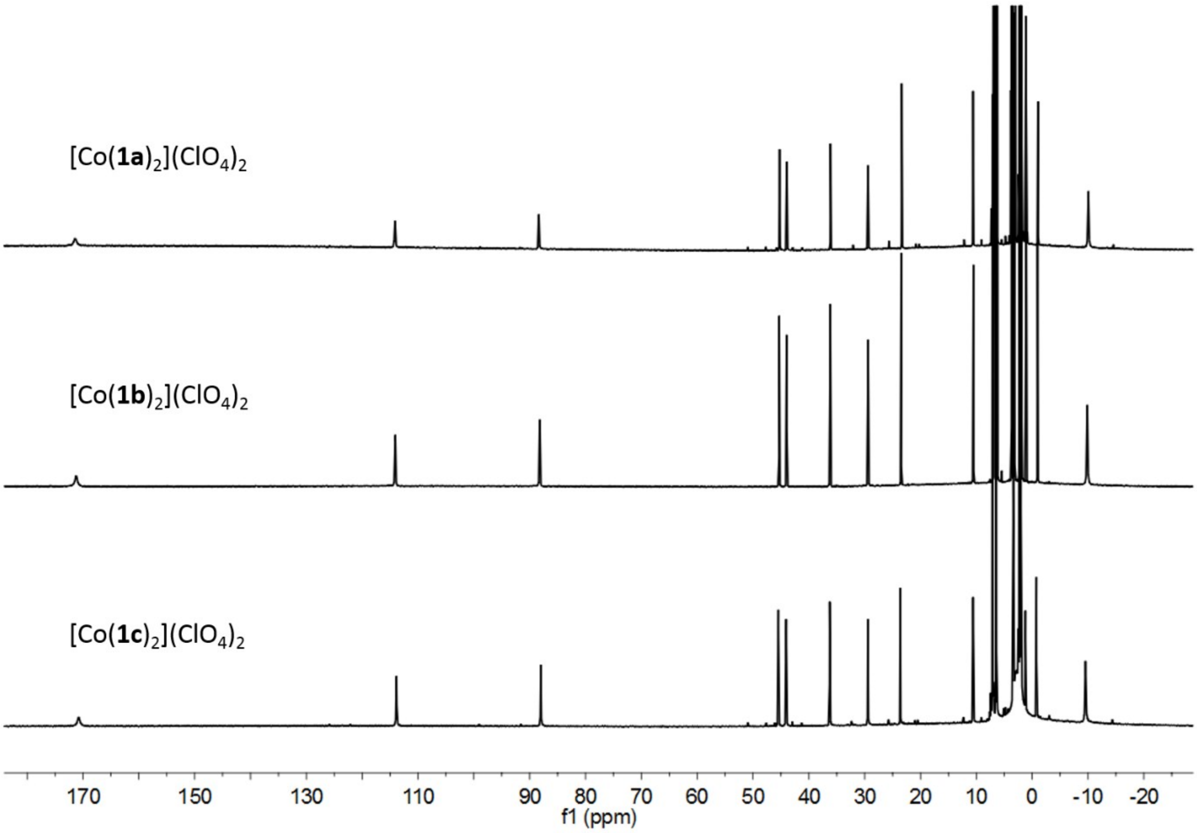

Figure 13-SI *^{1}H NMR spectra of complexes [Co(**1a-c**)$_2$](ClO$_4$)$_2$ in CD_3CN at T = 298 K.*

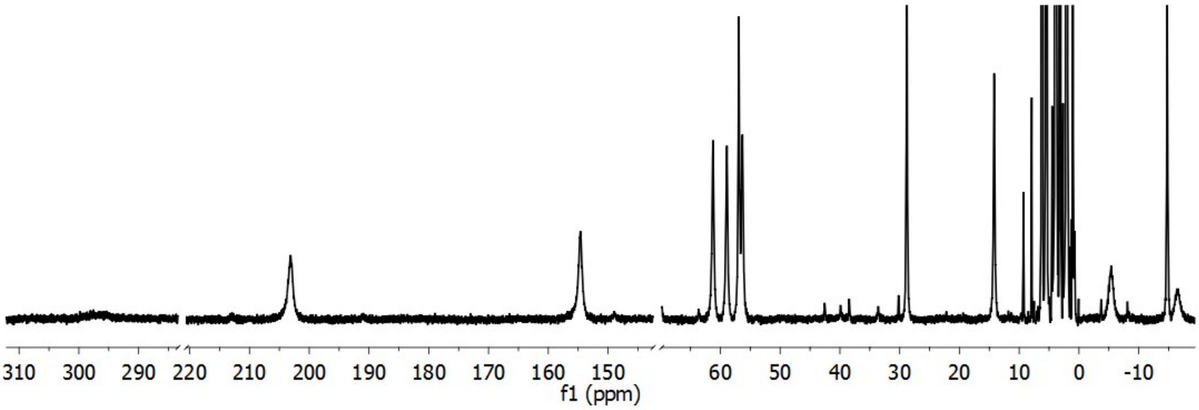

Figure 14-SI *^{1}H NMR spectrum of [Co(**1c**)$_2$](ClO$_4$)$_2$ in $(CD_3)_2CO$ at T = 193 K.*

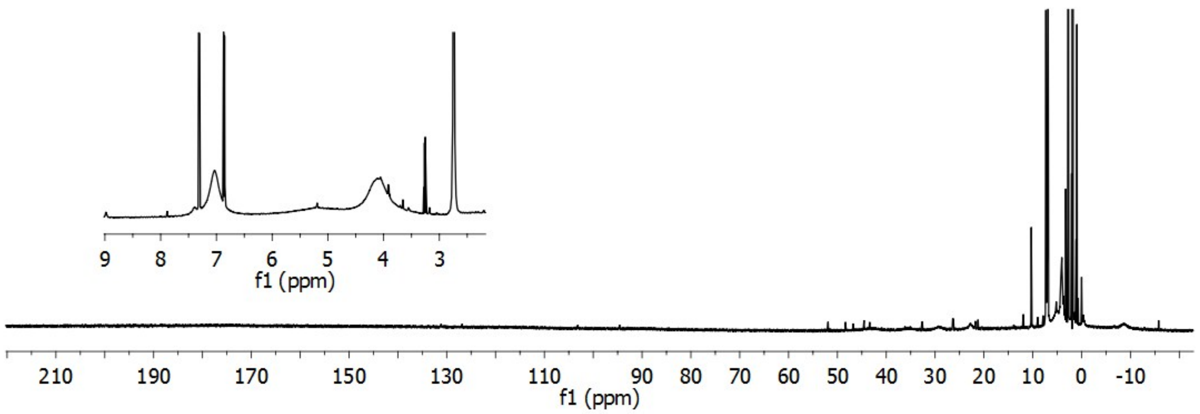

Figure 15-SI *^{1}H NMR spectrum of [Co^{2+}(**1c**)$_2$]$^{2+}$ which is partly oxidised using magic blue to [Co^{3+}(**1c**)$_2$]$^{3+}$ in (CD$_3$)$_2$CO at T = 298 K. The inset shows the broadened resonances of the anisyl protons. The reduced oxidants proton resonances are found at δ = 7.31 and 6.86 ppm.*

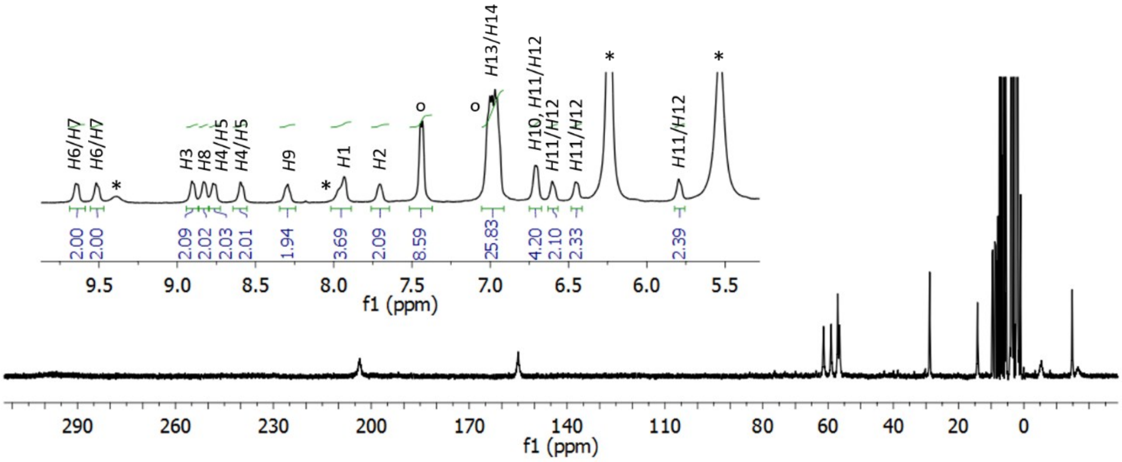

Figure 16-SI *^{1}H NMR spectrum of [Co^{2+}(**1c**)$_2$]$^{2+}$ which is partly oxidised using magic blue to [Co^{3+}(**1c**)$_2$]$^{3+}$ in (CD$_3$)$_2$CO at T = 193 K. The inset enlarges the section of aromatic proton resonances of the Co^{3+} species. The resonances marked with * are associated to the [Co^{2+}(**1c**)$_2$]$^{2+}$ complex, the two resonances marked with ^{0} are caused by the reduced oxidant N(p-C$_6$H$_5$Br)$_3$.*

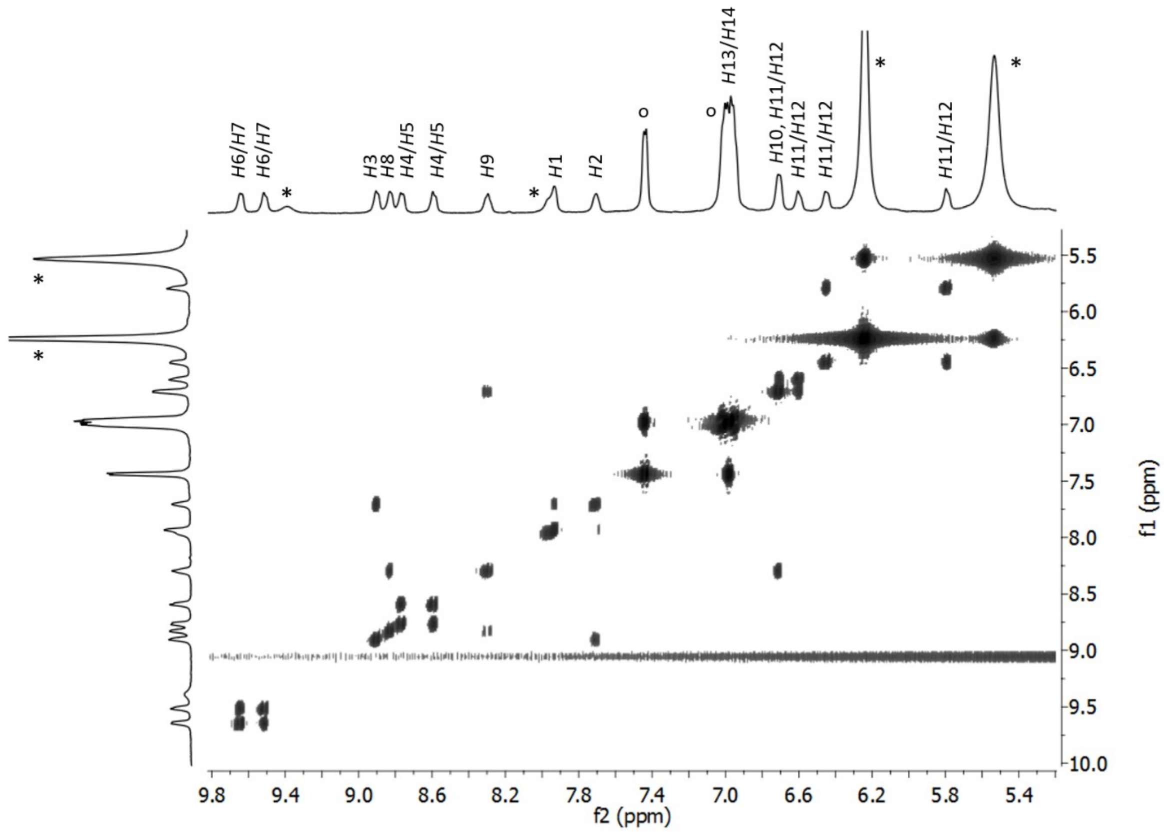

Figure 17-SI *Section of the $^1H,^1H$ COSY spectrum of in situ oxidised $[Co^{2+}(\mathbf{1c})_2]^{2+}$ to $[Co^{3+}(\mathbf{1c})_2]^{3+}$ by adding a sub-stoichiometric amount of magic blue in $(CD_3)_2CO$ at T = 193 K. The line-broadening is mainly due to the electron exchange between the HS-Co^{2+} and LS-Co^{3+} species. The * marked signals can be associated to the protons of the $[Co^{2+}(\mathbf{1c})_2]^{2+}$ species whereas the ^{0} marked signals are due to the reduced oxidant proton resonances.*

8. References

1 L. Schnaubelt, H. Petzold, J. M. Speck, E. Dmitrieva, M. Rosenkranz and M. Korb, *Dalt. Trans.*, 2017, **46**, 2690–2698.

2 C. Quinton, V. Alain-Rizzo, C. Dumas-Verdes, G. Clavier, F. Miomandre and P. Audebert, *European J. Org. Chem.*, 2012, 1394–1403.

3 N. M. O. Boyle, J. K. Pollock, M. Carr, A. J. S. Knox, S. M. Nathwani, S. Wang, L. Caboni, D. M. Zisterer and M. J. Meegan, *J. Med. Chem.*, 2014, **57**, 9370–9382.

4 Y. Li and T. Michinobu, *J. Polym. Sci. Part A Polym. Chem.*, 2012, **50**, 2111–2120.

5 S. M. Voshell and M. R. Gagné, *Organometallics*, 2005, **24**, 6338–6350.

6 F. Barrière and W. E. Geiger, *J. Am. Chem. Soc.*, 2006, **128**, 3980–3989.

7 A. Hildebrandt and H. Lang, *Organometallics*, 2013, **32**, 5640–5653.

8 D. Chong, J. Slote and W. E. Geiger, *J. Electroanal. Chem.*, 2009, **630**, 28–34.

9 R. J. LeSuer, C. Buttolph and W. I. Geiger, *Anal. Chem.*, 2004, **76**, 6395–6401.

10 H. J. Gericke, N. I. Barnard, E. Erasmus, J. C. Swarts, M. J. Cook and M. A. S. Aquino, *Inorganica Chim. Acta*, 2010, **363**, 2222–2232.

11 G. Gritzner and J. Kuta, *Pure Appl. Chem.*, 1984, **56**, 461–466.

12 I. Noviandri, K. N. Brown, D. S. Fleming, P. T. Gulyas, P. A. Lay, A. F. Masters and L. Phillips, *J. Phys. Chem. B*, 1999, **103**, 6713–6722.

13 J. R. Aranzaes, M.-C. Daniel and D. Astruc, *Can. J. Chem.*, 2006, **84**, 288–299.

14 M. Krejcik, M. Danek and F. Hartl, *J. Electroanal. Chem.*, 1991, **317**, 179–187.

15 A. Neudeck, A. Petr and L. Dunsch, *Synth. Met.*, 1999, **107**, 143–158.

16 F. Barrière, N. Camire, W. E. Geiger, U. T. Mueller-Westerhoff and R. Sanders, *J. Am. Chem. Soc.*, 2002, **124**, 7262–7263.

17 H. E. Gottlieb, V. Kotlyar and A. Nudelman, *J. Org. Chem.*, 1997, **62**, 7512–7515.